Spatial variation in estimation of shear key forces in segmented immersed tunnels

C.M.P 't Hart [1, 2], O. Morales-Nápoles [1], S.N. Jonkman [1]

[1] Delft University of Technology, Civil Engineering and Geosciences,
   Hydraulic Engineering, Delft, the Netherlands
[2] Royal HaskoningDHV, TEC, the Netherlands

Immersed tunnels are positive buoyant structures during installation and negative buoyant after installation. A tunnel is composed of sequential immersed elements that are coupled to each other in joints. Tunnel elements consist of segments which are compressed to each other by longitudinal post-tensioning. After immersion the tunnel is supported by the seabed and the longitudinal post-tension is cut at the joints between segments. Therefore, the structure is a segmented lining which is sensitive for settlements due to non-uniform circumstances over the length of the tunnel. An uneven response of the bedding underneath the tunnel introduces shear forces in joints of an immersed tunnel. Because immersed tunnels need to be buoyant during installation, they have limitations on weight and geometry, the size and therefore the capacity of these shear keys is limited because the height of the tunnel, as shear keys are applied in the walls of the tunnel. The foundation response is influenced by many factors related to subsoil but also to construction and dredging tolerances. The shear forces were derived as a function of different covariance lengths for subsoil stiffness and dredging tolerances for different tunnel layouts.

Keywords: Immersed tunnels, bedding, random fields, covariance length

1   Introduction

Immersed tunnels (IMT) are tunnels supported by a bedding of soft soil and a foundation layer. The majority of this type of tunnels is constructed by immersing prefabricated elements into a trench in the seabed. After finalization, the structure behaves as a lining of segments with lengths of about 20 to 25 m, that are connected by joints. Using this approach, the tunnel is less vulnerable to differential settlements, as the segment joints

only transfer shear forces via shear keys and large bending moments over the length of the structure are avoided. In the most common current design approach, an alternating bedding scenario along the tunnel axis is used as a conservative approach. (Reduction of the bedding stiffness of a single segment using a prescribed factor, as defined by Dutch requirements [1] and adopted for many tunnels worldwide.) However, this does not account for spatial variability in both the subsoil and the foundation layer below the tunnel. Instead, the current design approach is geometrically orientated on the tunnel to find the largest possible shear forces and not on the variability of the bedding support. This article presents a method to find the variability of forces in the shear key using Gaussian Random Fields (GRF), which are parameterized by a covariance length.

Using this method, more efficient, and more robust designs for immersed tunnels can be developed and can be identified as an alternative for the current design approach. The demonstrated model and method in this article also have limitations. For example, it assumes that the (internal and external) loads are uniform over the tunnel, as well as a continuous cross-sectional dimension in a straight line. In practice, curved, sloping elements with varying widths occur. Additionally, only 2 keys are considered per joint to transfer the shear forces, while in practice there could be more. Furthermore, in this paper a common gravel foundation is considered, noting that sand flow foundations are applied as well.

2   Literature

Different types of immersed tunnels (IMT) as well as their construction methods are discussed by Rasmussen et al. [2]. A general description of the IMT construction technique and a historical perspective is given by de Wit (2014) in [3] and design principles are described by Grantz (1997) [4]. A description of the development over the years is given by Glerum (1992) [5].

IMTs have traditionally a foundation of a gravel or a sand-flow foundation, both have their advantages and disadvantages, but differences between both methods were already described in 1978 by van Tongeren [6] and scale model tests on sand-flow were performed and researched by Li et al. (2014) [7]. The sand-jetting or sand-flow, was applied, for example on the Maastunnel in 1942 [8] and is highlighted by Glerum (1995) [9]. The gravel foundation was applied to the Øresund link between Copenhagen and Malmö.

60

Tunnels, not limited to IMT, rely on geotechnical as well as structural analysis. Random fields have been applied in a comparison study by Cheng (2019) [10] of a pressurized tunnel face of a bored tunnel and provides a practical design tool. Gong (2018) [11] presents a probabilistic analysis based on a random field generation for a longitudinal analysis for a bored tunnel. For a bored-tunnel section, a 2D plain strain approach including a random field generation is presented by Yu (2019) [12] in which the reliability of the tunnel lining is validated.

3   Nomenclature

Δt_{dl}	Dredging tolerance
Δt_{pl}	Gravel placement tolerance
α	Reduction factor alternating bedding
μ	Mean value
Σ	Covariance matrix
σ	Standard deviation
σ_a	Average contact pressure
σ_b	Bedding response
A_b	Contact area underneath the tunnel
F_i	Force at segment i
F_k	Absolute force at shear key
h_f	Foundation thickness
k_b	Bedding stiffness
k_f	Foundation material stiffness
k_s	Soil stiffness
L_{cov}	Covariance length [m]
L_s	Length of a segment
n_x	Number of points in x direction
n_y	Number of points in y direction
X	Location
x_n	x coordinate of point n [m]
y_n	y coordinate of point n [m]

4   Concepts

4.1   Immersed tunnels

Currently, the majority of IMTs are constructed using prefabricated elements of 100 to 150 m in a dry dock. The elements consist out of segments of 20 to 25 m which are compressed to each other for transportation by a posttensioning system. After casting and post-

tensioning the element, it is towed to the tunnel location and immersed into a dredged trench and laterally locked at its horizontal position using a back-fill and a protection layer (fig. 1). The sequentially immersed elements together form the total tunnel. After immersion, temporary post-tension is deactivated by cutting the tendons at the joints. As a result, a continuous flexible system is created and at the joints shear forces need to be transferred between segments (fig. 2). Structurally, in longitudinal direction the tunnel can be identified as a beam with hinges on an elastic bedding (fig. 3). Certain circumstances might give opportunity to keep the post-tensioning active and to have a monolithic system. In this paper, only a segmented structure is considered.
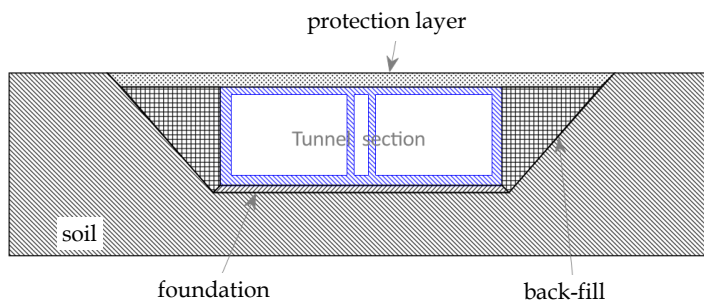
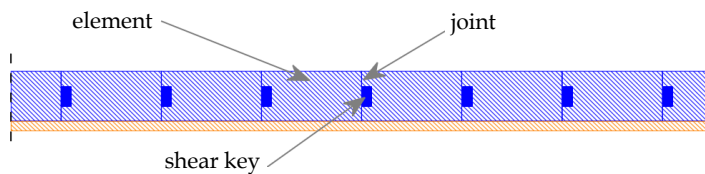Figure 1: Typical cross section of an immersed tunnel section

Figure 2: Typical longitudinal section of an immersed tunnel section
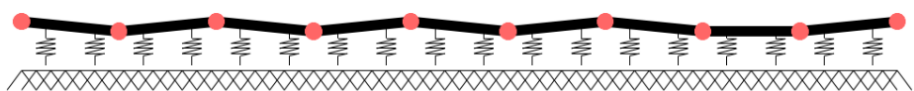

Figure 3: Typical longitudinal structural systems of Immersed tunnel – Hinged beam on bedding

The shear keys, which connect the segments provide a vertical shear capacity. A typical concrete shear key in a wall structure is presented together with a typical schematic reinforcement layout is presented in figure 4. The capacity is dependent on the size and material of the key. Adjustment of the key has its limitations. For example, as mentioned

before, the tunnel needs to be buoyant in the construction phase, adding material like thickening the key will influence this process. Furthermore, the key itself is obviously limited by the height of the tunnel.
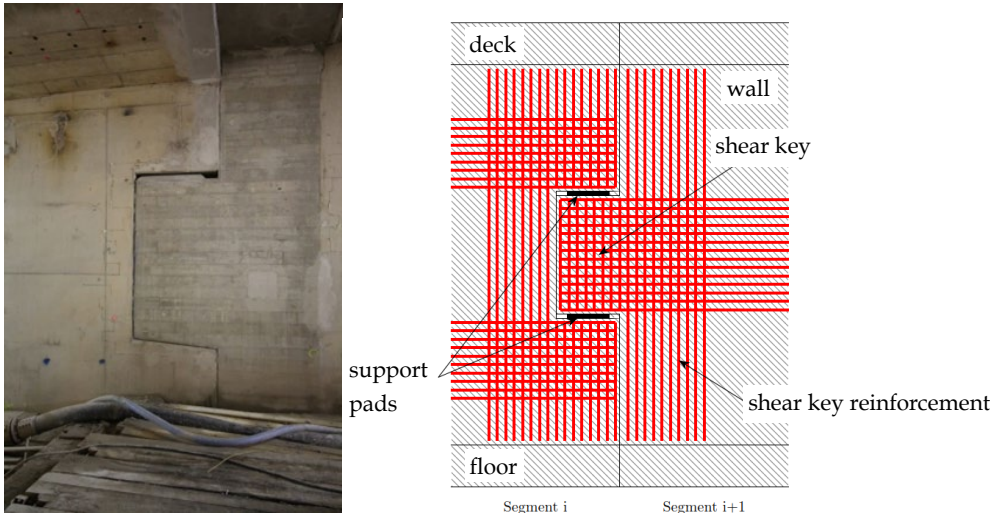

Figure 4: Concrete shear key in the Maasdeltatunnel (left) in an immersed tunnel and typical reinforcement layout (right)

Considerations for other materials has financial consequences. At the shear key location, a flexible joint is constructed and considered. Flexible joints are "weak" points in terms of water tightness of the tunnel and its number should be limited. In the current design approach of alternating bedding scenarios, longer distances between joints will increase the forces in the shear key.
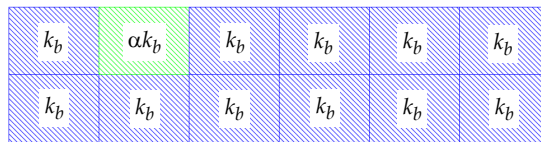
Variation in lateral direction
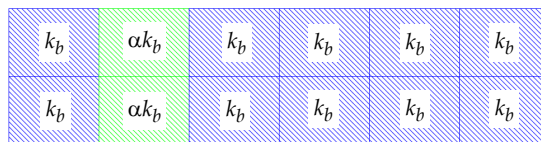
Variation in longitudinal direction

Figure 5: Alternating bedding

An optimal design would meet a segment length where the shear key is loaded to its maximum capacity. The results presented in this article are based on an analysis of a rectangular tunnel section using a gravel foundation, although the same approach as presented here can be used for a sand-flow foundation. In current designs, a conservative approach using a single reduction parameter on a segment foundation is applied in an alternating bedding stiffness (see figure 5 as sourced from [1]) where α is a reduction factor to be applied on the bedding stiffness in different scenarios to be considered.

4.2 *Gaussian random fields - spatial covariance*

The spatial covariance indicates that a local value of a particular parameter is correlated with neighbouring values of the same parameter depending on the spatial distance between locations. The distance between two points dictates to what extent the values on the two locations will vary. In this research Gaussian random fields (GRF) are applied to simulate the spatial variability. If a distance between 2 points increases, the covariance (statistical correlation) decreases exponentially. The covariance between two points in a grid is defined by the covariance length L_{cov} as expressed in equation 1.

$$\text{cov}((x_1,y_1),(x_2,y_2)) = \exp\left(-\frac{\sqrt{\pi}}{2}\frac{\sqrt{(x_2-x_1)^2+(y_2-y_1)^2}}{L_{cov}}\right) \tag{1}$$

To illustrate this dependency, for 3 hypothetical situations, three covariance length functions over distance have been plotted in figure 6. The actual covariance between individual locations is dictated by L_{cov} . If the covariance length is halved, the covariance between two points decreases faster; in contrast, if the covariance length is doubled, the covariance between two points decreases more slowly. If a surface is discretized
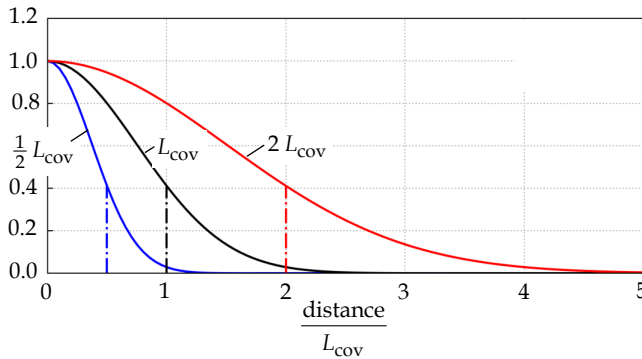

Figure 6: Covariance based on covariance length

to n_x times n_y , in which n_x is the number of points in the longitudinal direction and n_y in the lateral direction, the total number of points n is $n_x \cdot n_y$. The covariance matrix Σ contains the information regarding the covariance between all points within the grid defined by n_x and n_y . Factor $\frac{1}{2}\sqrt{\pi}$ in equation 1 is the scaling factor and can be adjusted for model representation.

If all distances between all points are available in a distance matrix, the covariance matrix Σ can be found in which for each connection the covariance is defined. Using equation 2, a multivariate Gaussian distribution be found, and samples can be generated given L_{cov} .

$$f_X(x_1,...x_n) = \frac{\exp(-\frac{1}{2}(x-\mu)^T \Sigma^{-1}(x-\mu))}{\sqrt{(2\pi)^n |\Sigma|}} \tag{2}$$

For an area of 100 × 100 m², 4 different samples are drawn using a Gaussian distribution (μ = 0, σ = 1 N/mm³) with different covariance lengths (1, 10, 100, 1000 m) in Figure 7. If the covariance length is very small compared to the area, a spike spatial distribution will be
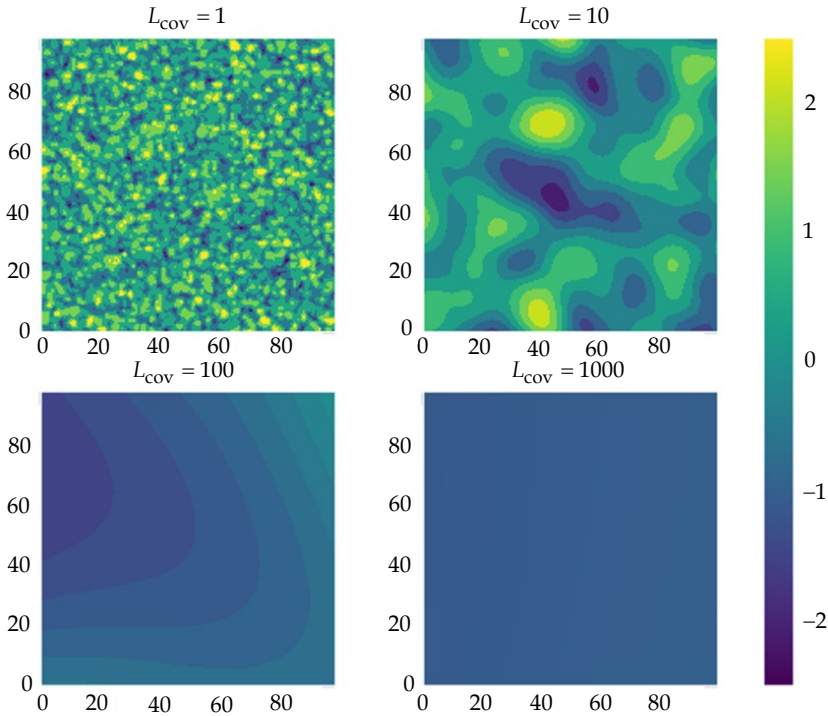

Figure 7: Spatial distributions for different covariance lengths

found whether there is hardly any correlation between points, if a large covariance length is used, there is hardly any variation over the area showing that there is a very strong correlation.

A sample of the field can then be transferred to any other distribution using a quantile transformation in which the quantiles of the normalized Gaussian distribution map to the quantiles of the target distribution. For the generation of GRF in this research, the GSTools, a toolbox for geostatistical modelling in Python is used [13].

The application of GRF is yet uncommon in designs of tunnel foundations. By nature, the soil parameters will develop continuously over the area. Special circumstances like faults and other exceptions will give raise to discrete transitions but are not considered in this research. The trench is dredged to immerse the tunnel in it; by itself the dredging process has a tolerance. After dredging, a layer of gravel is applied to the required level. The soil variables, such as stiffness, and the dredging level, which is directly related to the thickness of the foundation layer (fig. 8), are spatially correlated and can be described using GRF.

5 Model and analysis

In order to research the influence of the covariance length of both the subsoil and the dredging depth, an artificial representative model is constructed. The IMT is supported by the bedding, consisting of a subsoil and the foundation, and loaded with various loads acting on the tunnel. These loads will result in a bedding reaction underneath the IMT. The IMT is a concrete structure and has a significantly higher stiffness than the soil bedding.
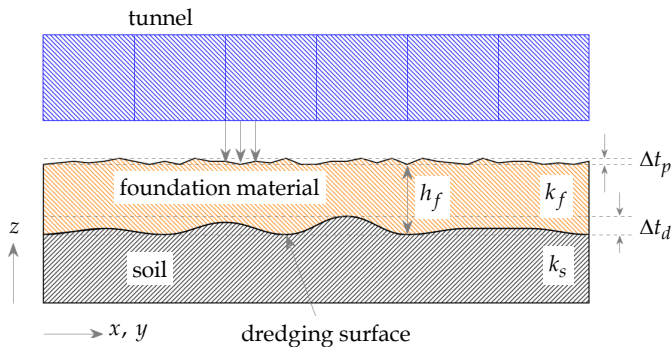

Figure 8: Bedding definition

As a result, the force distribution by the tunnel segment will be sensitive to bedding variations. Flexibility is induced to the tunnel along the longitudinal direction by the segment joints and the immersion or element joints. A base model of an IMT is used. The model has a length of 120 m and a width of 30 m. The segments are equally distributed over the length of the element and have individual segment lengths L_s of 20 m. A schematic overview is presented table 1.

Table 1: Element characteristics – base model

Element length	[m]	varies
Element width	[m]	30.0
Number of segments	[-]	6
Segment length	[m]	20

The six segments of the IMT are assumed to have a constant vertical displacement over the length of the considered tunnel part. The segments are considered as rigid bodies and the joints as flexible. Figure 9 shows the loading of the tunnel along the longitudinal direction.
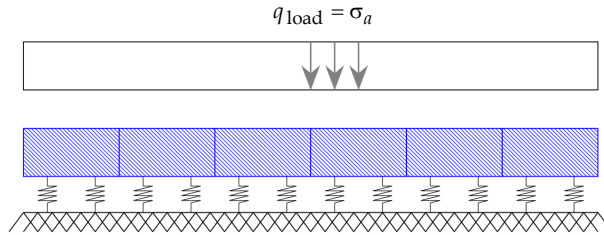

Figure 9: Tunnel system

The bedding is assumed to be elastic but, because of the spatial variability, not constant over the contact area of the tunnel. The linear stiffness of the subsoil is derived by a geotechnical analysis [1] and the bedding stiffness is then based on equation 3:

$$k_b(x,y) = \frac{1}{\dfrac{1}{k_s(x,y)} + \dfrac{h_f(x,y)}{k_f(x,y)}} \tag{3}$$

[1] A separate geotechnical analysis is required to derive the subsoil stiffness based on the geological layers, the soil characteristics and the influence depth of the tunnel.

where, h_f [m] is the thickness of the foundation material, k_f [N/m²] is the stiffness of the foundation material, Δt_d [m] is the dredging tolerance, Δt_p [m] is the placement tolerance and k_s [N/m³] is the subsoil stiffness (fig. 8).

In the final situation, after immersion and after applying the soil cover, an average compressing pressure σ_a is supplied to the foundation underneath the tunnel. The distributed load, on and in the tunnel, is adjustable by adding ballast weight and is based on vertical stability requirements. These requirements specify the minimal total resulting downward force to prevent floating up due to the buoyancy force. Because the bedding stiffness varies underneath the tunnel, the bedding response σ_b and therefore the load on the tunnel will vary over the contact area as presented in figure 10 and equation 4.

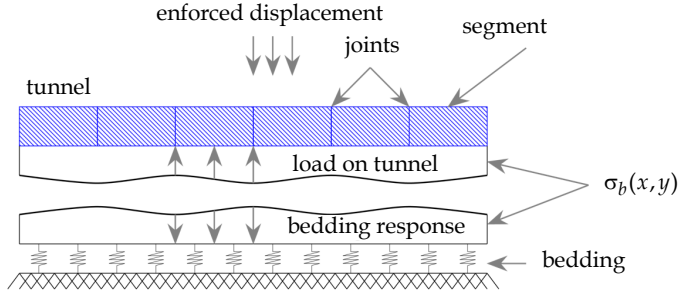$$\sigma_b(x,y) = k_b(x,y)\Delta u \tag{4}$$

Figure 10: Tunnel response

In this study, the vertical position of the tunnel is prescribed and adjusted in an iterative process until the average responsive stresses over the contact area A_b equals the load as described in equation 5.

$$\sigma_a = \frac{1}{A_b}\iint \sigma_b\,dx\,dy \tag{5}$$

It is assumed that the total element will have the same vertical displacement and remains undeformed, this is a conservative approach. In reality, the tunnel will deform slightly by small rotations of the segment and in the joints and, as a consequence, stresses will distribute between segments. If the stresses redistribute, the shear forces will reduce.

The bedding response variation leads to different stress distributions on the different segments. A shear force in a joint can be derived between two segments. Assuming the stiff IMT, the stresses will not redistribute between segments underneath the IMT and the

maximum shear forces between segments will be found. In this study an IMT with a two-shear key layout in the outer walls is assumed and each segment has therefore four shear keys. The sequence to derive the shear forces at a shear key after finding the equilibrium of the bedding response is presented in figure 11 and is obtained by:

- Integrate the stresses underneath each segment to get the total force on a segment (F_i).
- Find the center of gravity of the total force (red dots).
- Distribute the force to the shear key locations linearly (green dots).
- Define the shear key force as the absolute difference in forces between segments at the shear key locations ($F_{k,2-3}$ and $F_{k,1-4}$).
- Find the maximum shear key force of all shear keys.

In design, the maximum shear key force is used to compile a reinforcement layout for the shear key. In section 6 this sequence is repeated for both different covariance lengths and different geometrical tunnel layouts and is the covariance length related to the shear key force. With this method, a spatial variability of the bedding stiffness underneath the tunnel is considered. The variability not only differs in longitudinal direction of the tunnel but also in the lateral direction. In the presented model, only a spatial variation in subsoil stiffness and dredging depth are considered, besides that, the model also considers non spatial correlated variations such as variations in the top surface of the gravel and in the gravel stiffness. More parameters, spatial or non-spatial, can be varied in the model, such as settlements over time and gravel placement equipment.
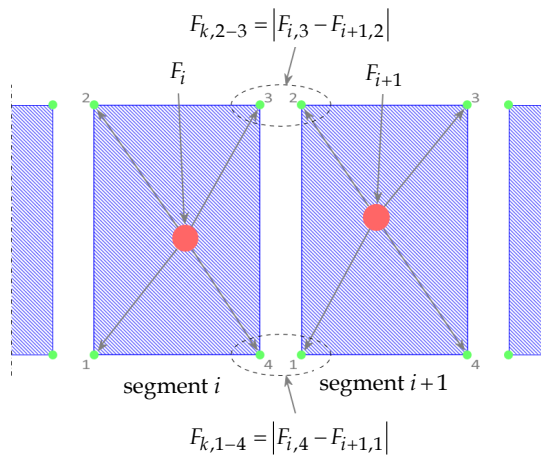

$$F_{k,2-3} = \left| F_{i,3} - F_{i+1,2} \right|$$

$$F_{k,1-4} = \left| F_{i,4} - F_{i+1,1} \right|$$

Figure 11: Force in a shear-key

6   Results

In this section, Monte Carlo analyses (n = 1000) are conducted in which the covariance lengths for both the soil stiffness as well as for the trench dredging are considered to be equal and fixed in each analysis. The generation of the variability of the subsoil stiffness and dredging depth are independent. An even stronger effect would have been found if the same GRF was used for both parameters, but this was considered less realistic as independent generation. In reality, not only the variability will be independent but also the covariance lengths of both parameters will be independent. However, to find a relation between covariance lengths and the shear key force, they are kept equal. Using this approach, the distribution of the shear force given the covariance length. In this demonstration model, the covariance lengths are considered independently. For the bedding variations the variable distributions as described in table 2 are used. These parameters are artificial and based on experience in several designs of various tunnels. In order to demonstrate the method, the quantity of the parameters is important as long as they are representative. For each sample, GRF are generated for both the subsoil stiffness as well as the thickness of the foundation layer based on the considered covariance length. The size of the GRF corresponds to the dimensions of the base model as shown in figure 8. Using the sequence specified in section 5, the maximum shear key force can be found in

Table 2: Parameters and distributions

Item	μ	σ	Distribution	Remarks
Gravel stiffness [kPa]	2000	300	Truncated Gaussian	uncorrelated
				min = 1000
				max = 3000
Soil stiffness [kPa]	5000	1600	Truncated Gaussian	min = 1800
				max = 8200
				L_{cov} = varies
Trench dredging or gravel thickness [m]	0.7	0.15	Truncated Gaussian	min = 0.35
				max = 1.05
				L_{cov} = varies
Gravel placement tolerance [mm]	0		Triangular	uncorrelated
				min = -10.0
				max = 15.0

each sample of the analysis and the total set result in a distribution of the maximum shear key force for a specific covariance length. The results are presented in figures 12 to 14. The following aspects can be identified:

- The maximum shear key forces (up to 4.8 MN) can be found if the covariance length is similar to the segment dimensions and the variation is larger.
- If the covariance length is small or large compared to the segment length, the maximum shear key force is small (with 1 to 1.5 MN) and shows a low variation.
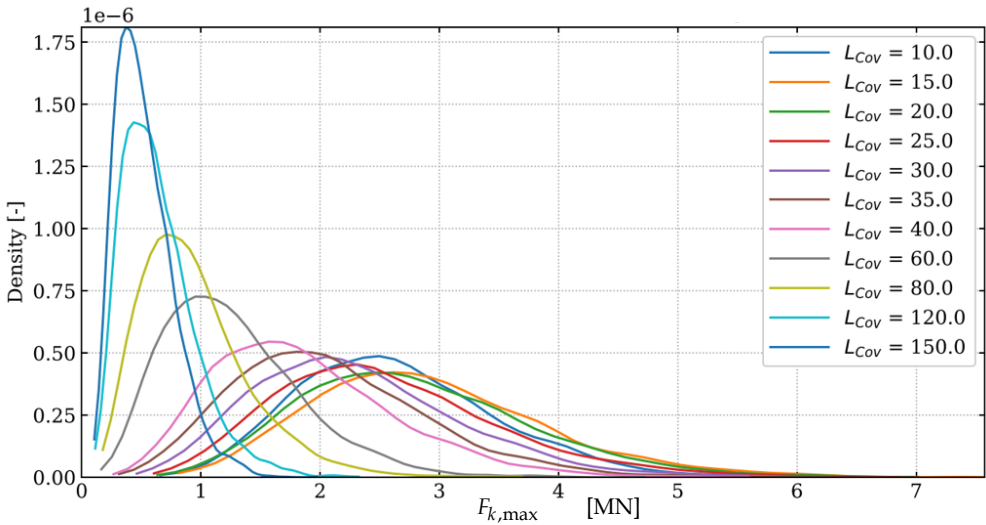

Figure 12: Distributions of the maximum shear key force for different covariance lengths, $n = 1000$, $L_S = 20$ m
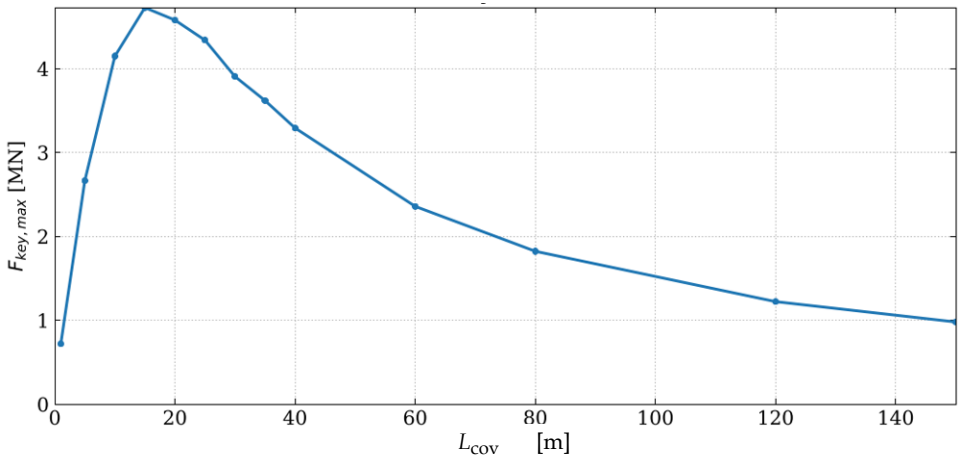

Figure 13: Shear key force at 95th percentile as function of the covariance length, $L_S = 20$ m

In figure 13, the relation between the shear key force at the 95th percentile of the distribution and the covariance length is shown. The 95th percentile is chosen as the characteristic design force. In design considerations for ultimate limit state evaluation this value is multiplied by a partial factor [14]. The maximum value of the force in shear key is found at around 16 m, before this value, the relation between force and length is positive after this value the relation is negative. The value is considered as the split value.
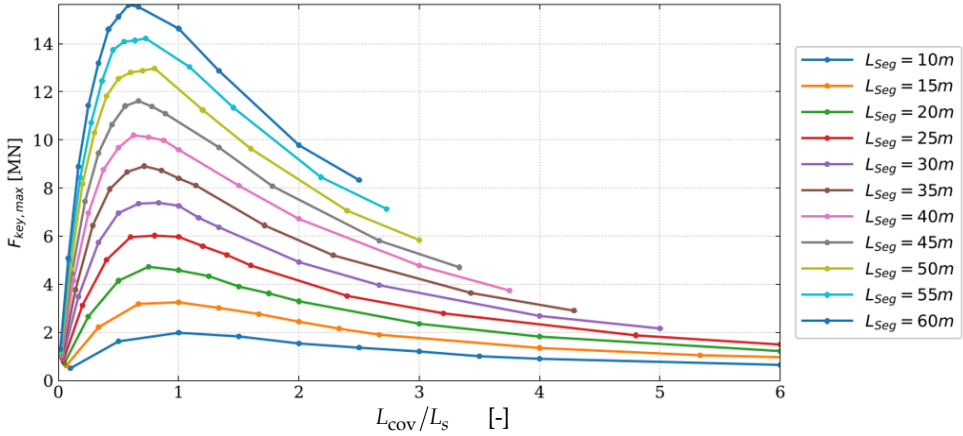

Figure 14: Shear key force at 95th percentile as a function of the covariance length for different segment lengths
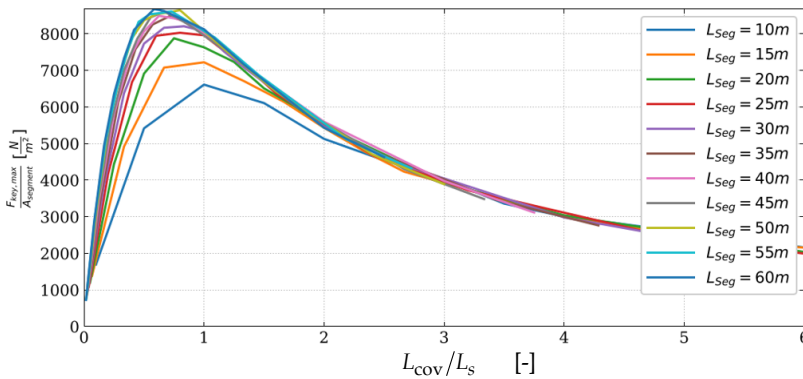

Figure 15: Relative shear key force at 95th percentile as a function of the covariance length for different segment lengths

In figure 12 the number of segments and the width of the tunnel are constant. In figure 14 the segment length L_s is varied from 10 to 60 meter, while keeping the number of segments

72

equal to 6 (which changes the total element length), so the total contact area under tunnel varies with the different segment length. On the horizontal axis the covariance length is divided by the segment length for comparison. The results are plotted for the covariance length over the segment length and the shear key force found at the maximum density as presented in figure 12. Figure 15 shows the same figure as figure 14, but for comparison, F_k is divided by the contact area $A_{segment}$ under the segment. The following observations can be made from figure 14:

- F_k increases with the segment length L_s . Larger integration areas, due to the increase of L_s , underneath a segment will cause higher shear forces which can exceed the capacity of a shear key.
- The maximum F_k is found if the segment dimensions (length and width) and L_{cov} are similar.
- If L_{cov} increases to larger values compared to L_s , the F_k decreases.

There appears a strong relation between the covariance length and the shear key force. Secondly, as a geometrical consequence of a smaller area below the segment, smaller segment lengths show smaller shear key forces. An optimization of the segment length could be discussed, as joints are weaker spots in terms of water tightness. But in reality, the segment length depends on other factors as well, such as the casting sequence, seasonal temperature loads introducing longitudinal effects and so on. However, the conclusion gives useful input in the early stage of the design of the geometry and structural solutions.

7 Relation to traditional design

In the more traditional design approach with the alternating bedding, the stiffness is considered uniform underneath a segment and a segmented beam on an elastic foundation is used to describe the model behavior. To account for torsional effects and consequently varying shear forces in the keys in one joint, a factor is used which usually is taken as 20% to 25% of the shear force found. Variation of the bedding along the tunnel is accounted for by an alternating bedding which is specified by a factor depending on the foundation construction method. In the alternating bedding approach, no spatial variation in the subsoil is considered and it is independent of the dredging method. In reality, this will vary by the marine environment and depth.

The 3D method presented in this paper differs substantially from the current 2D design approach. Both methods require soil investigation and interpretation of these results. If the soil investigation is intensified, both models will have an increasing accuracy but only on the subsoil stiffness. Nevertheless, if a covariance length or an interval of covariance lengths can be derived, a distribution of shear forces can be derived. In case the covariance length cannot be derived based on the available soil investigations, an upper bound for the covariance lengths can be found in an estimation of the maximum value for the forces in the shear key. An interval around the split value will give an upper bound distribution of the shear key forces.

8   Conclusion and discussion

In this research, a method is presented to establish a relation between spatial variation of subsoil and dredging parameters and the shear key forces in IMT. Considering the relation between the covariance lengths and the shear key forces, the following conclusions can be drawn:

- The largest shear key forces are found, when the covariance length is of the same order as the segment length of the tunnel.
- The absolute shear key force increases with the segment length.

The latter conclusion is obvious; the area of a segment over which the stresses are integrated is larger and will lead to larger forces.

Based on these conclusions, the design of the segment length can be optimized, if the covariant lengths are known or estimated within limits, for example by more intensive soil investigation using cone penetration testing (CPT) or quality measures and monitoring of the dredging process. If possible, it should be avoided in the design to have segment lengths that are almost the same as the covariant lengths. However, the shear key force does not only depend on the segment length. DeGroot et al. [15] presents a method for estimating covariance lengths. The thickness of the foundation material is based on the dredging tolerance. One could think of extending the quality measures or the dredging method to improve the dredging accuracy, because it would lead to a more constant thickness and stiffness and therefor a lower variability on the stiffness of the foundation layer. However, in daily practice, the selection of the dredging method depends on marine conditions and geology. The dredging method also dictates the dredging tolerance. As an

74

extra option, by changing the thickness of the foundation layer, the influence of the subsoil stiffness on the bedding stiffness can be decreased.

In this research, only covariance lengths for the soil stiffness and dredging depth are considered and both parameters are considered the same. The latter could be topic of discussion, if the top part of the soil influences the dredging process, a correlation between both could appear. However, if the soil consists out of a multi-layer profile, this influence of the top layer on the total stiffness of the soil will reduce. In order to use this method in the design process for tunnels and even parts of the method can be used. The GRF model can be used to derive bedding stiffness to adopt in longitudinal analyses and transverse analyses. When the subsoil stiffness and the thickness of the foundation layer are inputted including their covariance lengths, or the most conservative covariance lengths (close to the segment dimensions), distributions of average bedding stiffness per segment can be derived. In reality, the soil characteristics will vary also over the support area of the tunnel. The application of the method needs adjustment, where the applicable distribution of the soil parameters develops over the area. Usually, different CPTS are taken over the area. Different stiffness subsoil characterizations can be found over the support area. It is up to the designer how to account for these differences as the characterization of the subsoil stiffness can be assumed continuous or with discrete transitions. Both options can be served using the quantile transformation to the quantiles of the local subsoil distribution. In this method demonstration, the shear force is transferred over two keys. In this way, the distribution of the shear key force is statically defined. However, tunnel can be supplied with more shear keys, if needed. To account for a distribution, a design can assume that the tunnel segment will remain undeformed and that the shear forces will linearly distribute between two segments. If the support conditions on the segments are assumed as springs, a contribution from the segment to the shear keys can be derived. Subtracting the forces from two segments will lead to the individual shear forces for each shear key. A general assumption here is that the segments will behave independently. This assumption is valid as long as the segments will behave similarly. If the stiffness between bedding differs substantially between segments as for example at faults or at the transition to cut & cover sections, this cannot be assumed.

As a recommendation for further research, more parameters should be part of the scope. Additionally, the parameters used in this study are all based on a distribution with a fixed

set of parameters. This could represent a single situation, however, to draw more robust conclusions it is recommended to extend further research with, but not limited to:

- Multiple layers of subsoil
- Settlements
- Dredging scenarios or methods
- Non uniform loading
- Variation of IMT geometry
- Different segment lengths over the tunnel length
- More than 2 keys in the segment joint
- Interaction between 2 elements

9 Further research

The method proposed in this article, including a probabilistic approach, has been first published in 2024 [16]. In the probabilistic approach a dataset of 3 variables is compiled. For the generation, two different situations have been considered, one in which the covariance lengths are smaller than the split value shown in figure 13. Using two probabilistic methods, Non-Parametric Bayesian Networks and Regular Vines, exceedance probabilities are calculated which can be related to requirements set by local codes and standards.

References

[1] RWS, 2017. Richtlijn Ontwerp Kunstwerken v1.4. Ministerie van Infrastructuur en Milieu.

[2] Rasmussen, N.S., 1997. Concrete immersed tunnels — forty years of experience. *Tunnelling and Underground Space Technology* 12, 33–46. URL: https://www.science direct.com/science/article/pii/S0886779896000612, doi:https://doi.org/10.1016/S0886-7798(96)00061-2.

[3] de Wit, J., van Putten, E., 2014. The immersed tunnel as fixed link – a successful alternative pushed by innovation. Proceedings of the *World Tunnel Congress*.

[4] Grantz, W., 1997. Chapter 3 structural design of immersed tunnels. *Tunnelling and Underground Space Technology* 12, 93–109. doi:10.1016/S0886-7798(97)90015-8.

[5] Glerum, A., 1992. Options for tunneling: a personal story. *Tunnelling and Underground Space Technology* 7, 313–315. URL: https://www.sciencedirect.com/science/article/pii/088677989290059Q, doi:https://doi.org/10.1016/0886-7798(92)90059-Q.

[6] van Tongeren, H., 1978. The foundation of immersed tunnels. Proceedings of *Delta Tunneling Symposium* , 48–57.

[7] Li, W., Fang, Y., Mo, H., Gu, R., Chen, J., Wang, Y., Feng, D., 2014. Model test of immersed tube tunnel foundation treated by sand-flow method. *Tunnelling and Underground Space Technology* 40, 102–108. URL: https://www.sciencedirect.com/science/article/pii/S0886779813001454, doi:https://doi.org/10.1016/j.tust.2013.09.015.

[8] Gravesen, L., Rasmussen, N.S., 1993. A milestone in tunnelling: Rotterdam's maas tunnel celebrates its fiftieth anniversary. *Tunnelling and Underground Space Technology* 8, 413–424. URL: https://www.sciencedirect.com/science/article/pii/088677989390003E, doi:https://doi.org/10.1016/0886-7798(93)90003-E.

[9] Glerum, A., 1995. Developments in immersed tunnelling in holland. *Tunnelling and Underground Space Technology* 10, 455–462. URL: https://www.sciencedirect.com/science/article/pii/088677989500031S, doi:https://doi.org/10.1016/0886-7798(95)00031-S.

[10] Cheng, H., Chen, J., Chen, R., Chen, G., 2019. Comparison of modeling soil parameters using random variables and random fields in reliability analysis of tunnel face. *International Journal of Geomechanics* 19, 04018184. doi:10.1061/(ASCE)GM.1943-5622.0001330.

[11] Gong, W., Juang, C., Martin, J., Tang, H., Wang, Q., Huang, H., 2018. Probabilistic analysis of tunnel longitudinal performance based upon conditional random field

simulation of soil properties. *Tunnelling and Underground Space Technology* 73, 1–14. doi:10.1016/j.tust.2017.11.026.

[12] Yu, X., Cheng, J., Cao, C., Li, E., Feng, J., 2019. Probabilistic analysis of tunnel liner performance using random field theory. *Advances in Civil Engineering* 2019, 1–18. doi:10.1155/2019/1348767.

[13] Müller, S., Schüler, L., Zech, A., Heße, F., 2022. GSTools v1.3: a toolbox for geostatistical modelling in python. *Geoscientific Model Development* 15, 3161–3182. URL: https://gmd.copernicus.org/articles/15/3161/2022/, doi:10.5194/gmd-15-3161-2022.

[14] for Standardization, E.C., 2002. EN 1990. Eurocode: Basis of structural design. CEN, Brussels.

[15] DeGroot, D., Baecher, G., 1993. Estimating autocovariance of in-situ soil properties. *Journal of Geotechnical Engineering* 119. doi:10.1061/(ASCE)0733-9410(1993)119:1(147).

[16] 't Hart, C.M.P. Morales-Nápoles O., Jonkman, S.N., The influence of spatial variation on the design of foundations of immersed tunnels: Advanced probabilistic analysis, *Tunnelling and Underground Space Technology*, Volume 147, 2024.

[17] Hicks, M.A., Li, Y., 2018. Influence of length effect on embankment slope reliability in 3d. *International Journal for Numerical and Analytical Methods in Geomechanics* 42, 891–915. URL: https://onlinelibrary.wiley.com/doi/abs/10.1002/nag.2766, doi:https://doi.org/10.1002/nag.2766, arXiv:https://onlinelibrary.wiley.com/doi/pdf/10.1002/nag.2766.